NUMERICAL STUDY ON ZONE PLATE IMAGING*

Y.W. Parc, I.S. Ko[#], POSTECH, Pohang, Republic of Korea
J. Y. Huang, PAL, Pohang, Republic of Korea

Abstract

The electron beam will be imaged by two zone plates in 1B2 beamline to measure electron beam size in the Pohang Light Source (PLS). From numerical study, we can determine the optical limit of resolution for Fresnel zone plates with the same specifications in the 1B2 beamline. The width of the Airy pattern and the outmost width of the zone plate turn out not to be good parameters to determine the resolution of the imaging system with a zone plate. The resolution of the entire imaging system 1B2 beamline will be 682 nm.

INTRODUCTION

X-ray imaging with a Fresnel zone plate (FZP) has the potential to show the best resolution in the imaging of electron beams [1, 2]. The authors in Ref. [1] estimate the expected resolution of a zone plate as 0.55 μm. They estimate the resolution from the width of the Airy pattern without any numerical study of the diffractogram. However, the distribution of the diffractogram from a point source is different from an Airy pattern: in particular, the width of the highest peak in the diffractogram is narrower than the Airy pattern. We can get better resolution than that estimated from the width of Airy pattern. We need to numerically study the imaging phenomena to determine the resolution accurately.

In this paper, we present a numerical study to understand the imaging of the electron beam with two FZPs. From this study, the effect of the width of diffractogram to the resolution of the imaging system is clearly understood. The numerical study to understand the imaging of electron beam with zone plate is presented in Section 2. Definitions on the resolution of the imaging system using zone plate are discussed in Section 3. The summary is provided in Section 4.

NUMERICAL STUDY

In this section, a numerical study to understand the zone plate imaging is presented. The principle of X-ray imaging using a zone plate will be explained. The configuration for zone plate imaging of electron beam is shown in Figure 1.

The electron distribution in the electron bunch is now assumed as a Gaussian distribution as in

$$B(\xi) = \frac{1}{\sigma\sqrt{2\pi}} \exp\left(-\frac{\xi^2}{2\sigma^2}\right) \qquad (1)$$

where ξ is the coordinate to describe the electron bunch distribution and σ is the standard deviation of the Gaussian distribution. In this numerical study, this standard deviation is 35 μm for the vertical beam size in PLS which is reported by the author [3].
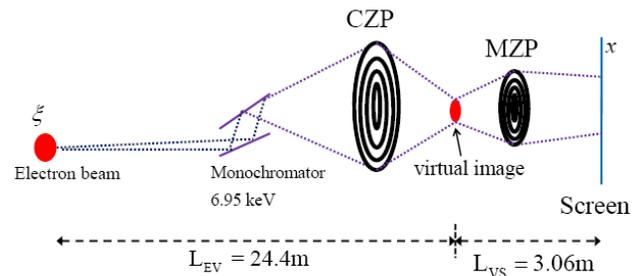

Figure 1: Schematic view of X-ray imaging at 1B2 beam line in Pohang Light Source (PLS). The energy of X-ray after monochromator is 6.95 keV. The distance from the electron beam to the virtual image L_{EV} is 24.4 m. The distance from the virtual image to the detector L_{VS} is 3.06 m. The vertical electron beam σ is about 35 μm.

Virtual image from condenser zone plate (CZP)

The design of a CZP at 1B2 beamline is drawn in Fig. 3(a). In this design, it is assumed that radiation source exists at infinitely long distance from the CZP. The radius from center to a zone of the CZP is denoted as r_n where n is named as zone number. The radiation propagates from the zone makes constructive interference with that propagates from the center of the CZP at the screen. Maximum of the zone number is denoted by N. Note that total number of the open zones is $N/2$. The formula to calculate the focal length is derived as shown:

$$f_C = \frac{r_N^2 - N^2\lambda^2/4}{N\lambda} \qquad (2)$$

where f_C is the focal length of the CZP and λ is the wavelength of the X-ray. The total number (N) of the zones is 10001 for the CZP in 1B2 beamline. The radius of the outmost zone (r_N) is 2 mm. The width of the outmost zone ($\Delta r_N \equiv r_N - r_{N-1}$) is 100 nm. The focal length (f_C) of the CZP in the 1B2 beamline is 2.2569 m.

The schematic configuration for the imaging of electron beam by the CZP is shown in Fig. 3(b). The image of best resolution is not formed at the focal length. The image of the electron beam is constructed at the longer position from the CZP, which position will be called the imaging point in this study. The length from the CZP and the imaging point is defined as imaging length denoted by L_{CV}. The imaging of electron beam at the imaging length is not measured in this study. The image made by the CZP is defined as virtual image in this study. This virtual image is assumed as a new radiation source to the MZP in this numerical study.
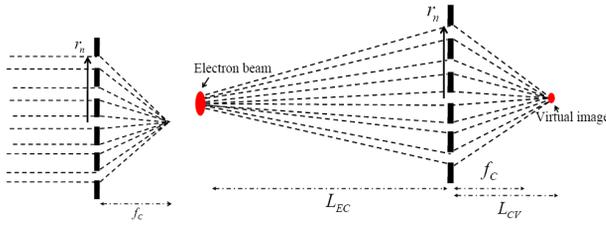

Figure 3: (a, *left*) Design of CZP. The focal length is 2.2569 m. The zone number N is 10001. The radius of the outmost ring (r_N) is 2 mm. (b, *right*) Schematic view for the virtual imaging of electron beam by CZP.

The relation between the focal length and the optimal imaging length is given in Ref. [1]:

$$f_C = \frac{1}{1/L_{EC} + 1/L_{CV}} \tag{3}$$

With relation in Eq. (2), we can calculate the optimal imaging length:

$$L_{CV} = \frac{L_{EV} - \sqrt{L_{EV}^2 - 4L_{EV}f_C}}{2} = 2.5163\,\text{m} \tag{4}$$

In Figure 4(a), a diffractogram with the smallest width is shown by solid line when the length L_{CV} is 2.5163 m. There is one highest peak in the central part and are two small peaks at the both sides. All other parameters used in the numerical study are same with experimental condition that was shown in Figure 1. The position of the zero intensity of the second high peak is almost matched with the first zero position of Airy pattern which is shown by dotted line [4]. The position of the zero intensity of the second high peak is 0.20 μm. The position of the first zero intensity of Airy pattern is also the same. However, we cannot use simply the width of Airy pattern as a resolution of the imaging as used in Ref. [1]. Detail discussion will be given in Section 3.

In Figure 4(b), the numerically calculated virtual image of the electron beam with 6.95 keV radiation is shown by

solid line. The dashed line is the plot of Eq. (1) multiplied by the magnification M_C defined as

$$M_C = \frac{L_{CV}}{L_{EC}} = \frac{2516300}{21883700} = 0.115$$

The dashed line in Fig. 5(b) is considered as expected virtual image of the electron beam. The half width of the half maximum (HWHM) of the expected virtual image is calculated as

$$HWHM_{virtual} = M_C \sigma \sqrt{2\ln 2} = 4.7385\,\mu\text{m}$$

The virtual image obtained from numerical calculation is shown in Fig. 5(b) with solid line. The HWHM of the virtual image in Fig. 5(b) is 4.753 μm. The virtual image obtained by numerical study is slightly wider than the expected virtual image. The resolution of imaging using a CZP will be discussed in the next section.
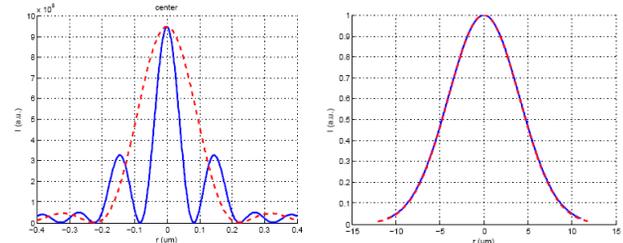

Figure 4: (a, *left*) Diffractogram with point source; (b, *right*) Virtual image obtained from numerical study. L_{CV} = 2.5163 m, L_{EV} = 21.8837 m.

Real image from microzone plate (MZP)

The design of the MZP at 1B2 beamline is drawn in Figure 5(a). f_M is the focal length of the MZP. Total number (N) of the zones is 571 in the CZP. The radius outmost zone is 80 μm. The width of the outmost zone is 70 nm. The focal length (f_M) of the MZP is calculated from Eq. (2) as 63.55 m.

The schematic configuration for the imaging of the virtual image by the MZP is shown in Figure 5(b). The virtual image formed by the CZP is used as a new radiation source for the MZP imaging in this numerical study. The length between the MZP and the imaging point is denoted by L_{VM}.
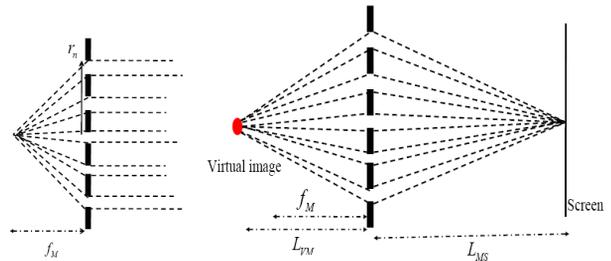

Figure 5: (a, *left*) Design of MZP. The focal length is 63.55 mm. The zone number is 571. The radius of the outmost ring (r_N) is 80 μm. (b, *right*) Schematic view for the imaging of electron beam on the screen by MZP.

The optimal imaging length of the MZP is also calculated with similar formula with Eq. (4),

$$f_C = \frac{1}{1/L_{VM} + 1/L_{MS}} \qquad (3)$$

$$L_{VM} = \frac{L_{VS} - \sqrt{L_{VS}^2 - 4L_{VS}f_M}}{2} = 0.0647\,\text{m}$$

In Fig. 6(a), a diffraction pattern with the smallest width is shown by solid line. The length L_{VM} is 64.7 mm. The overall shape of this diffraction pattern is similar with the case shown in Fig. 4(a). However, the width of the diffractogram is wider than that of diffraction shown in Fig. 4(a).

In Fig. 6(b), the numerically calculated X-ray image of the electron beam with 6.95 keV radiation generated is shown by solid line. The dashed line is the expected image by the magnification M defined as

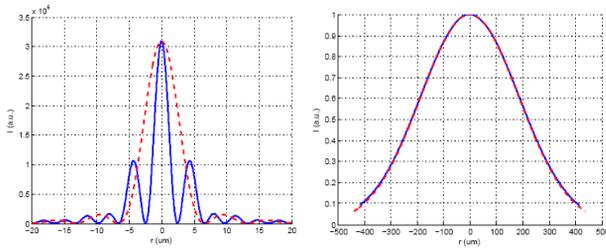$$M_M = \frac{L_{MS}}{L_{VM}} = \frac{2.9953}{0.0647} = 46.295$$

Figure 6: (a, left) Diffractogram with point virtual source (b, right) Image on the screen obtained from numerical study. L_{VM} = 64.720mm, L_{MS} = 2.995280 m.

The final magnification can be estimated with

$$M = \frac{L_{EC}}{L_{CV}}\frac{L_{VM}}{L_{MS}} = 0.115 \times 46.295 = 5.324$$

The size image in the screen will be 5.324 times larger than the real electron beam size in PLS.

The vertical beam size is 38.6 ± 0.58 μm. This result is quite similar to the result reported in Ref. [3] by the authors of this paper.

The half width of the half maximum (HWHM) of the expected image on the screen is calculated as

$$HWHM_{image} = M_M M_C \times HWHM_{electron}$$

$$= M\sigma\sqrt{2\ln 2} = 219.4\,\text{μm}$$

If we use the HWHM (4.7530 μm) of the expected virtual source in the numerical study, the HWHM of the numerical image on the screen is 220.9 μm not shown here. The expected image is well matched with the numerically obtained image in this case. However, as we can see in above subsection, the virtual image is slightly larger than the expected one. We use the HWHM (4.7384 μm) of the virtual source in the numerical study. The HWHM of the image on the screen is 221.5 μm as shown in Fig. 8(b). This value should be compared with the experimentally measured vertical beam size.

SUMMARY

To prepare for the measurement of electron beam size with zone plates, the image of the X-ray light using zone plates is studied numerically. A conventional definition of resolution shows differences from the result from numerical study. A new definition of total resolution of the imaging system is proposed. The total resolution in X-ray imaging at 1B2 beamline in PLS will be 682 nm.

REFERENCES

[1] K. Iida, N. Nakamura, H. Sakai, K. Shinoe, H. Takaki, M. Fujisawa, H. Hayano, M. Nomura, Y. Kamiya, T. Koseki, Y. Amamiya, N. Aoki, and K. Nakayama, Nucl. Instrum. Methods Phys. Res., Sect. A 506, 41 (2003).

[2] H. Sakai, M. Fujisawa, K. Iida, I. Ito, H. Kudo, N. Nakamura, K. Shinoe, T. Tanaka, H. Hayano, M. Kuriki, and T. Muto, Phys. Rev. ST Accel. Beams 10, 042801 (2007).

[3] Y. W. Parc, J. Y. Huang and I. S. Ko, J. Synchrotron Radiat. resubmitted (2011)

[4] M. Born and E. Wolf, Principles of Optics (Cambridge University Press, New York, 1999), 7th ed. (extended), p. 437.